Supporting Information

Morphology Control of Stimuli-Responsive Fluorescence-Enhanced Supramolecular Aggregates Based on Pillar[5]arene

Xuejia Gan[a+], Peng Liu[a+], Yingying Deng[a+], Qingqing Han[a], Jinghua Yin[a]*, Long Yi Jin[a]*

Department of Chemistry, National Demonstration Centre for Experimental Chemistry Education, Yanbian University, Yanji 133002, P. R. China

[+]*Contributed equally to this work*

**To whom correspondence should be addressed.*

L. Y. Jin, E-mail: jhyin@ybu.edu.cn, lyjin@ybu.edu.cn, Telephone: +86-04332732997

1. Experiment

1.1 General Materials

hydroquinone, potassium carbonate, acetonitrile, sodium azide, dimethyl sulfoxide, 1,4-bis(bromomethyl)benzene, propargyl bromide, magnesium chloride, triethylamine, paraformaldehyde, sodium borohydride, dichloromethane, methanol, ethyl 4-bromobutyrate, boron trifluoride diethyl etherate, 1,6-dibromohexane, acetone, tetraethylene glycol, tetrahydrofuran, sodium hydride, p-toluenesulfonyl chloride, hydrochloric acid, sodium hydroxide.

1.2 Instruments

^{1}H-NMR (300 MHz) and ^{13}C-NMR (75 MHz) spectra were recorded on a Bruker AM-300 instrument. ^{1}H-NMR (500 MHz) and ^{13}C-NMR (125 MHz) spectra were recorded on a Bruker AM-500 instrument. MALDI-TOF-MS was performed on a PerSeptive Biosystems Voyager-DESTR instrument using 2-cyano-3-(4-hydroxyphenyl) acrylic acid (CHCA) as the matrix. The Uv-vis and FL spectra were obtained with JASCO UV-V650 UV-vis and FP-8200 FL spectrometers, respectively. Transmission electron microscope (TEM) experiments were performed with a JEOL 2010Plus microscope.

1.3 Theoretical simulation

The complex was subjected to rigorous Density Functional Theory (DFT) calculations with a focus on molecular optimization. All atoms were treated using the

B3LYP/6-311G** method. To further elucidate its properties, molecular dynamics simulations were performed using the Materials Science Maestro software package.

2. Synthesis and Characterizations

2.1 Synthesis of the molecules 1-10, H_2, H_3

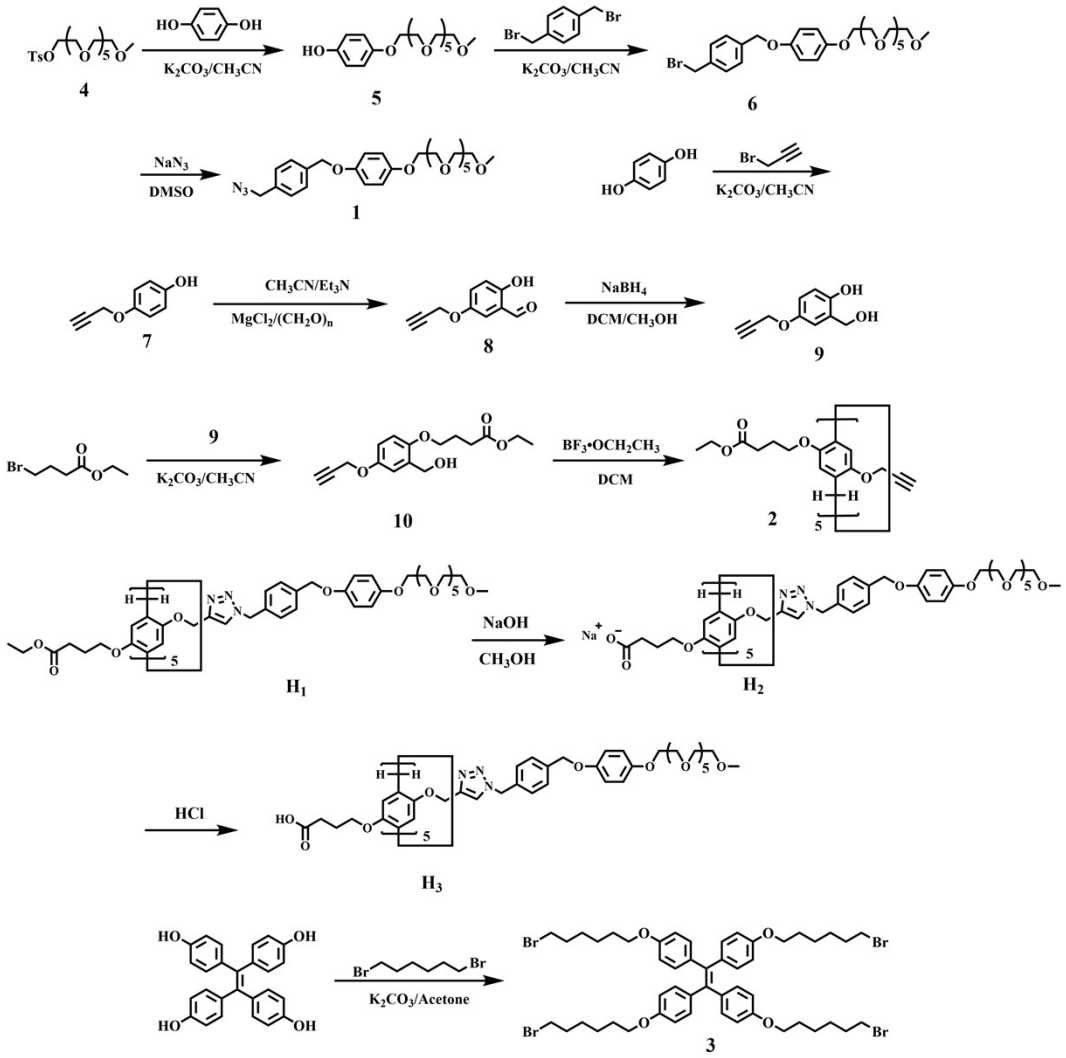

Scheme S1 Synthetic routes of **1-10**, H_2, H_3.

The intermediates of **2-10** were prepared according to the references described Elsewhere.[S1,S2]

Compound **4**: ^{1}H NMR (300 MHz, $CDCl_3$, δ, ppm): 7.80 (d, J = 8.2 Hz, 2H), 7.32 (t,

J = 15.0 Hz, 2H), 4.30 - 4.06 (m, 2H), 3.83 - 3.46 (m, 22H), 3.38 (s, 3H), 2.45 (s, 3H).

Compound **5**: ^{1}H NMR (300 MHz, $CDCl_3$, δ, ppm): 6.90 - 6.61 (m, 4H), 4.19 - 3.97 (m, 2H), 3.90 - 3.78 (m, 2H), 3.77 - 3.44 (m, 20H), 3.38 (s, 3H).

Compound **6**: ^{1}H NMR (300 MHz, $CDCl_3$, δ, ppm): 7.39 (s, 4H), 6.95 - 6.73 (m, 4H), 4.99 (s, 2H), 4.49 (s, 2H), 4.15 - 4.00 (m, 2H), 3.88 - 3.78 (m, 2H), 3.77 - 3.46 (m, 20H), 3.37 (s, 3H).

Synthesis of **1**: Into a 100 mL single-neck round-bottom flask was added sodium azide (0.35 g, 5.38 mmol), followed by the addition of DMSO (15 mL). The mixture was stirred until complete dissolution was achieved, after which **6** (1.447 g, 2.54 mmol) was added. The reaction mixture was stirred in a water bath at room temperature for over 12 hours. Finally, added an appropriate amount of water, extracted, and washed 3-5 times with saturated sodium chloride solution. Purification by column chromatography (silica gel, 100-200 mesh) afforded 1.20 g of **1** in an approximate yield of 88.67%. ^{1}H NMR (300 MHz, $CDCl_3$, δ, ppm): 7.45 (d, *J* = 8.0 Hz, 2H), 7.33 (d, *J* = 8.1 Hz, 2H), 6.97 - 6.77 (m, 4H), 5.02 (s, 2H), 4.35 (s, 2H), 4.14 - 4.01 (m, 2H), 3.89 - 3.79 (m, 2H), 3.79 - 3.46 (m, 20H), 3.38 (s, 3H).

Compound **7**: ^{1}H NMR (300 MHz, $CDCl_3$, δ, ppm): 6.92 - 6.84 (m, 2H), 6.84 - 6.72 (m, 2H), 4.63 (d, *J* = 2.4 Hz, 2H), 3.63 (s, 1H), 2.50 (t, *J* = 2.4 Hz, 1H).

Compound **8**: ^{1}H NMR (300 MHz, $CDCl_3$, δ, ppm): 10.70 (s, 1H), 9.87 (s, 1H), 7.30 - 7.20 (m, 1H), 7.14 (d, *J* = 3.0 Hz, 1H), 6.96 (d, *J* = 9.0 Hz, 1H), 4.70 (d, *J* = 2.3 Hz, 2H), 2.55 (t, *J* = 2.2 Hz, 1H).

Compound **9**: ^{1}H NMR (300 MHz, DMSO, δ, ppm): 8.94 (s, 1H), 6.93 (s, 1H), 6.67 (d, *J* = 1.6 Hz, 2H), 4.99 (t, *J* = 5.6 Hz, 1H), 4.65 (d, *J* = 2.4 Hz, 2H), 4.55 - 4.35 (m, 2H), 3.49 (t, *J* = 2.3 Hz, 1H).

Compound **10**: ^{1}H NMR (300 MHz, $CDCl_3$, δ, ppm): 6.97 (d, *J* = 2.9 Hz, 1H), 6.90 - 6.69 (m, 2H), 4.65 (d, *J* = 2.6 Hz, 4H), 4.27 - 4.09 (m, 2H), 4.06 - 3.92 (m, 2H), 2.63 - 2.39 (m, 3H), 2.20 - 2.03 (m, 2H), 1.35 - 1.12 (m, 3H).

Compound **2**: ^{1}H NMR (300 MHz, $CDCl_3$, δ, ppm): 6.96 - 6.53 (m, 2H), 4.81 - 4.29 (m, 2H), 4.28 - 3.96 (m, 2H), 3.96 - 3.54 (m, 4H), 2.56 (s, 2H), 2.08 (d, *J* = 22.2 Hz, 3H), 1.41 - 0.84 (m, 3H).^{13}C NMR (75 MHz, $CDCl_3$, δ, ppm): 173.27, 151.50, 148.76, 128.79, 128.19, 115.40, 114.66, 79.33, 74.78, 67.42, 60.41, 56.38, 31.18, 25.14, 14.24.

Synthesis of $\mathbf{H_{2\text{-}3}}$: A methanolic solution of compound H_1 was treated with an aqueous sodium hydroxide solution and heated to 70 ℃ with stirring for 12 h. The reaction mixture was then acidified with hydrochloric acid, extracted, and concentrated under reduced pressure to afford compound $\mathbf{H_3}$. Then, sodium hydroxide aqueous solution was added to $\mathbf{H_3}$ until completely dissolved, yielding $\mathbf{H_2}$ aqueous solution. Molecule $\mathbf{H_3}$: ^{1}H NMR (300 MHz, DMSO-d_6, δ, ppm): 8.29 (s, 5H), 7.35 (s, 25H), 6.87 (s, 25H), 5.65 (s, 5H), 5.47 (s, 5H), 5.05 - 4.58 (m, 20H), 3.98 (s, 10H), 3.69 (s, 10H), 3.66 - 3.45 (m, 60H), 3.44 - 3.35 (m, 60H), 3.22 (s, 15H), 2.01 (s, 10H), 1.86 (s, 10H). ^{13}C NMR (75 MHz, $CDCl_3$, δ, ppm): 176.73, 153.21, 152.88, 150.35, 149.30, 144.77, 137.81 , 134.48, 134.30, 128.59, 128.29, 128.10, 123.34, 123.17, 115.68, 115.60, 71.90, 70.74 , 70.55, 70.47, 69.99, 69.82, 67.98, 59.01, 53,81, 30.69, 24.97. MALDI-TOF-MS:

m/z calculated [M]: 3901.8; found: $[M]^+$: 3924.2.

Compound **3**: ^{1}H NMR (300 MHz, $CDCl_3$, δ, ppm): 6.90 (d, *J* = 1.8 Hz, 8H), 6.62 (d, *J* = 8.2 Hz, 8H), 3.90 (d, *J* = 8.1 Hz, 8H), 3.42 (t, *J* = 6.8 Hz, 8H), 2.02 - 1.83 (m, 8H), 1.83 - 1.67 (m, 8H), 1.49 (d, *J* = 7.0 Hz, 16H).

2.2 ^{1}H NMR spectra of of molecules 1-10

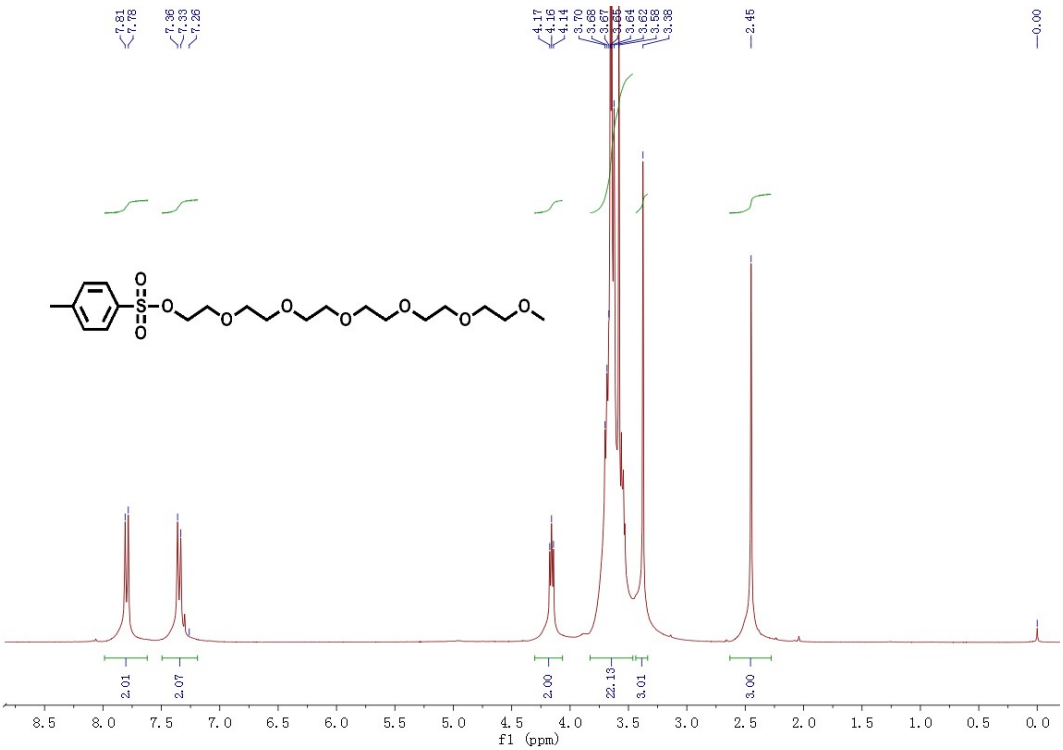

Figure S1 ^{1}H-NMR spectrum of molecule **4** in $CDCl_3$.

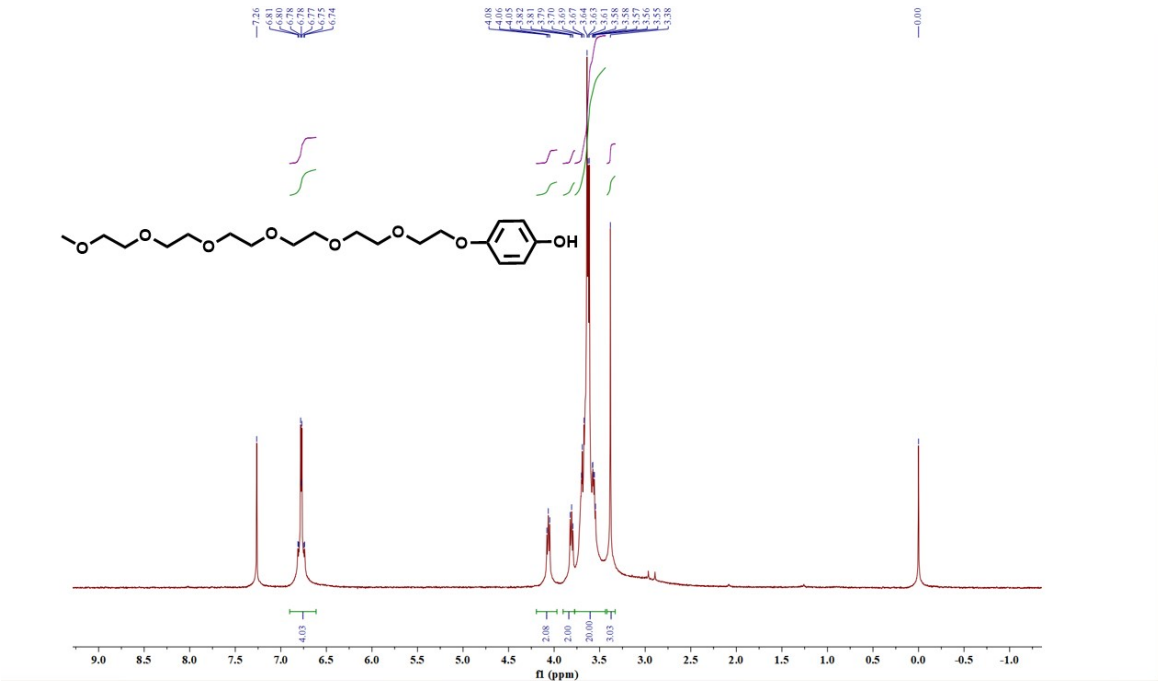

Figure S2 ^{1}H-NMR spectrum of molecule **5** in $CDCl_3$.

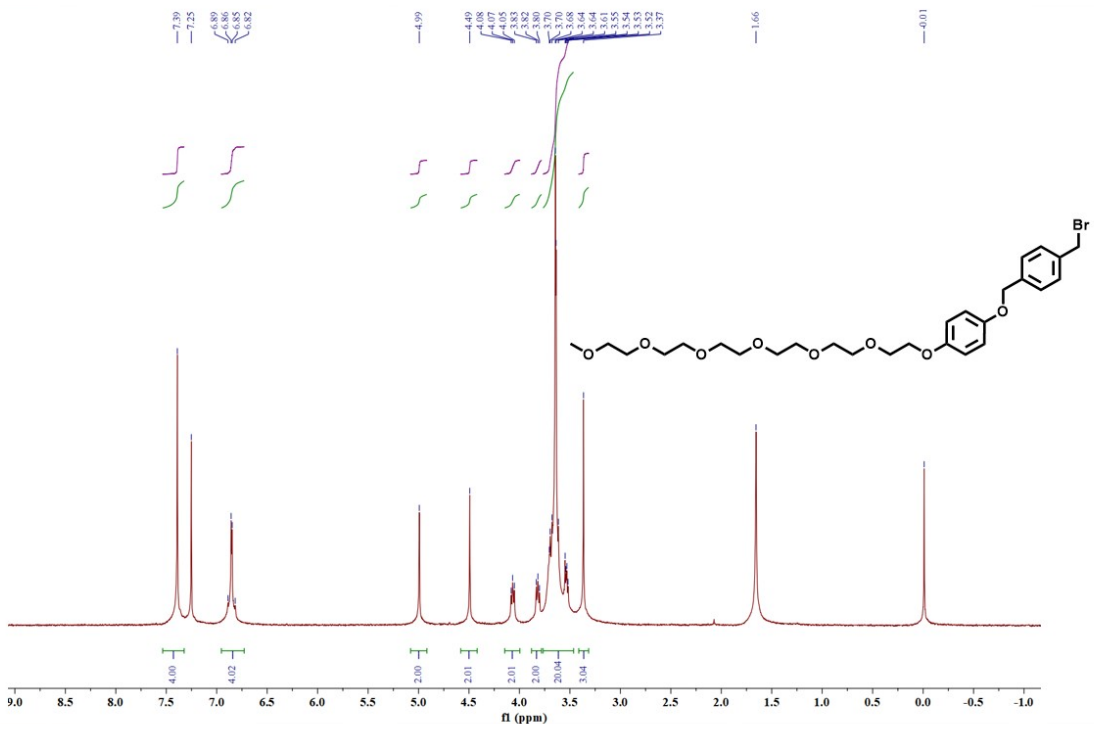

Figure S3 ^{1}H-NMR spectrum of molecule **6** in $CDCl_3$.

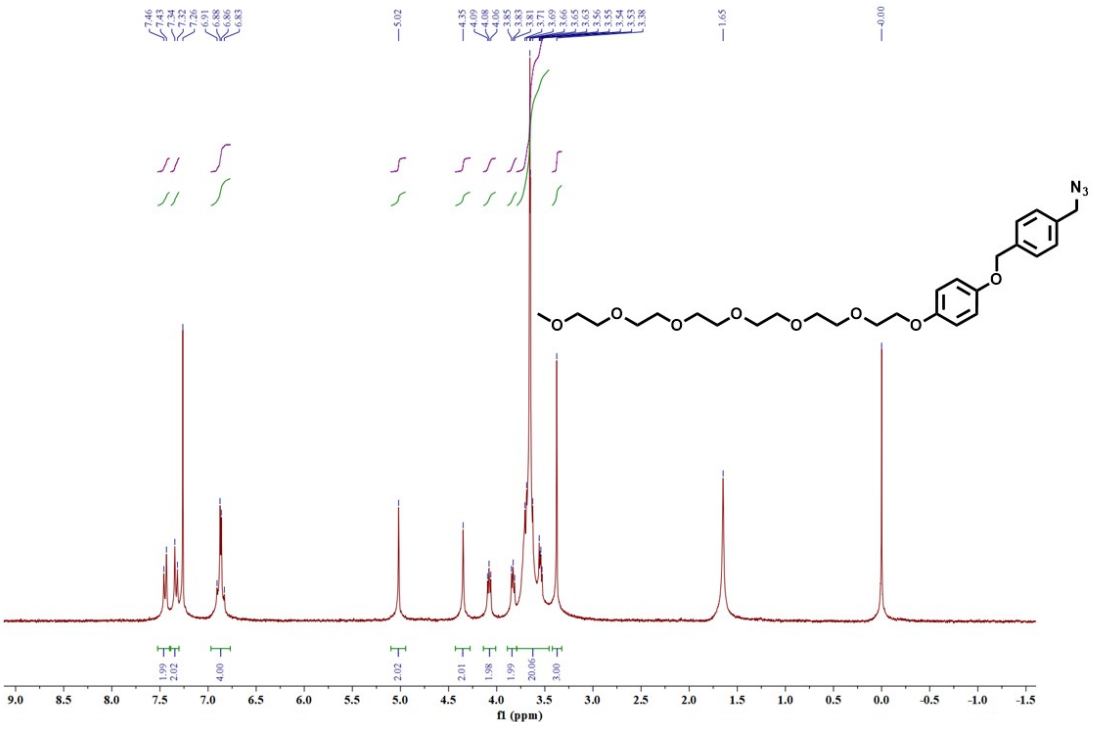

Figure S4 ^{1}H-NMR spectrum of molecule **1** in $CDCl_3$.

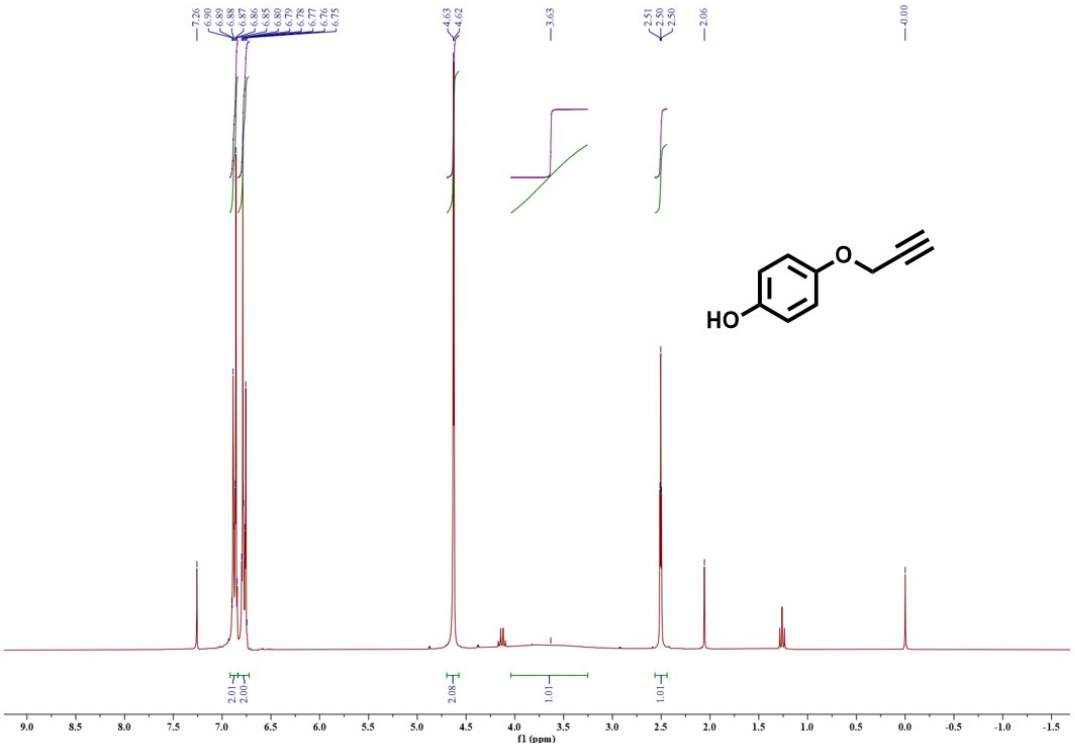

Figure S5 ^{1}H-NMR spectrum of molecule **7** in $CDCl_3$.

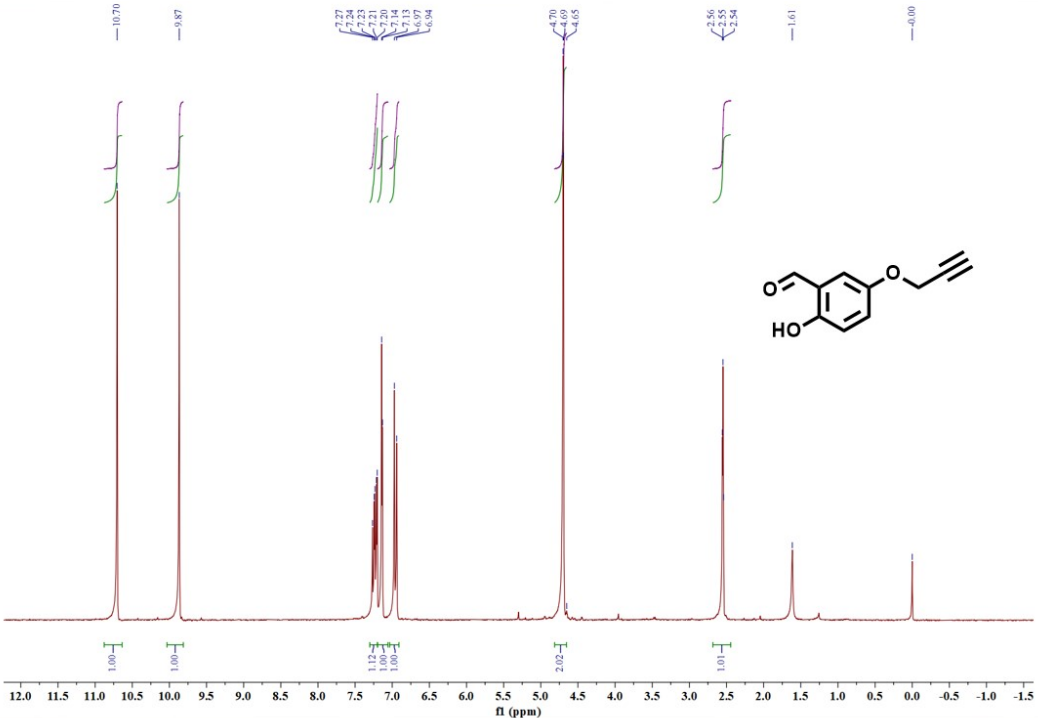

Figure S6 ^{1}H-NMR spectrum of molecule **8** in $CDCl_3$.

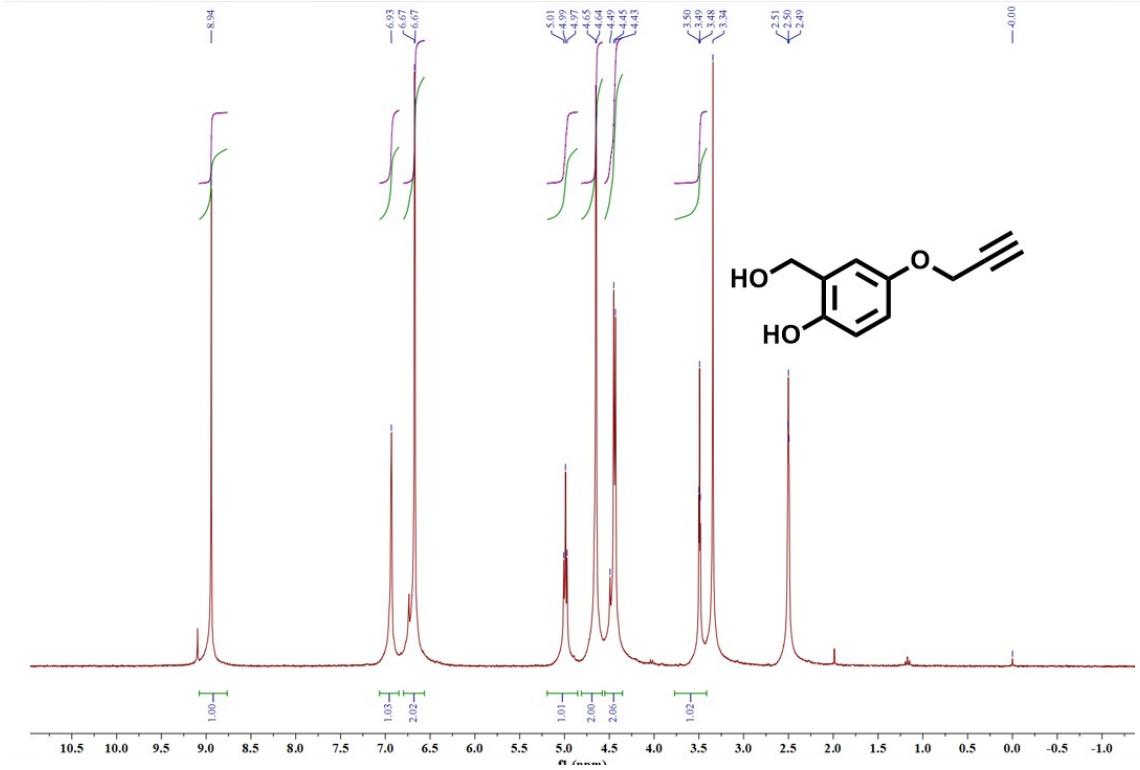

Figure S7 ^{1}H-NMR spectrum of molecule **9** in DMSO-d_6.

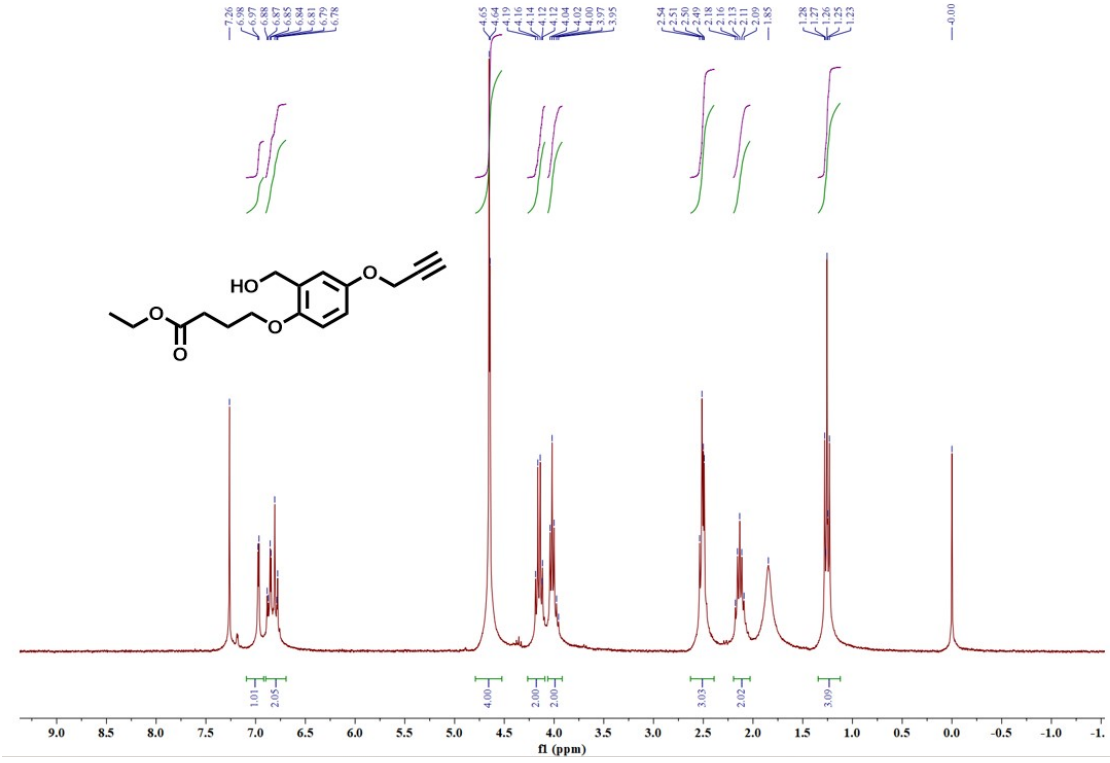

Figure S8 ^{1}H-NMR spectrum of molecule **10** in $CDCl_3$.

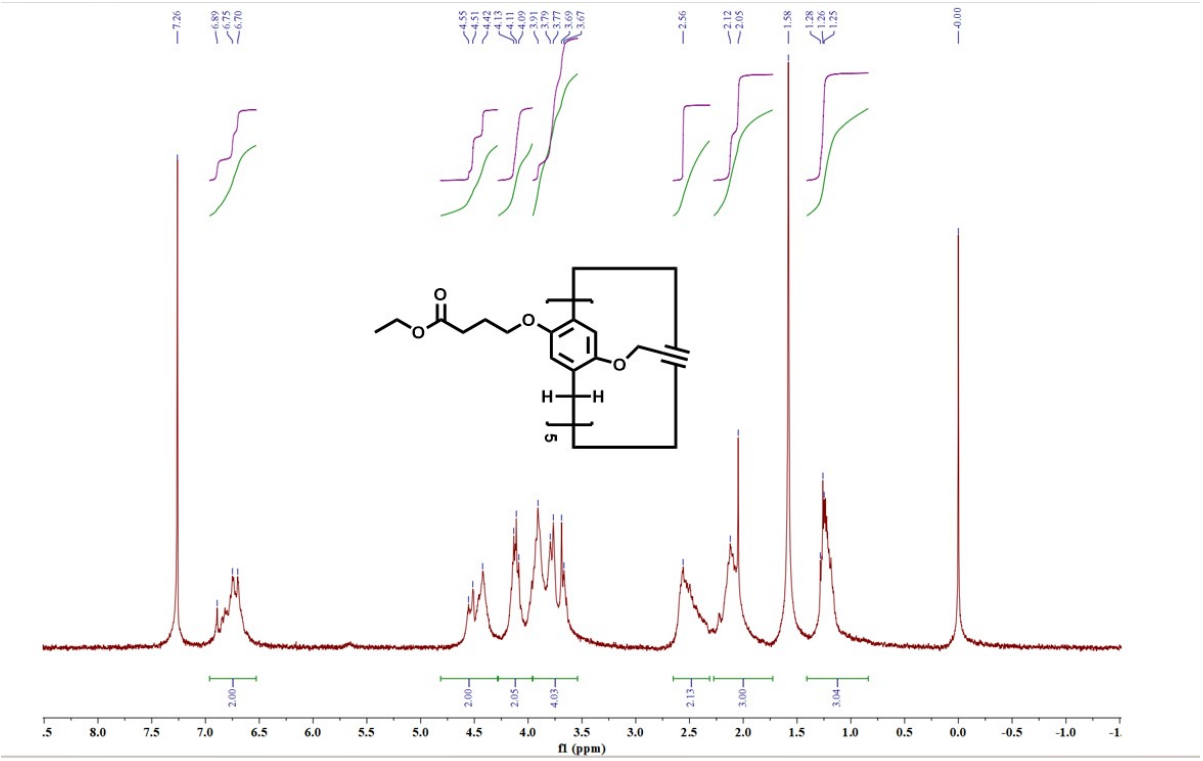

Figure S9 ^{1}H-NMR spectrum of molecule **2** in $CDCl_3$.

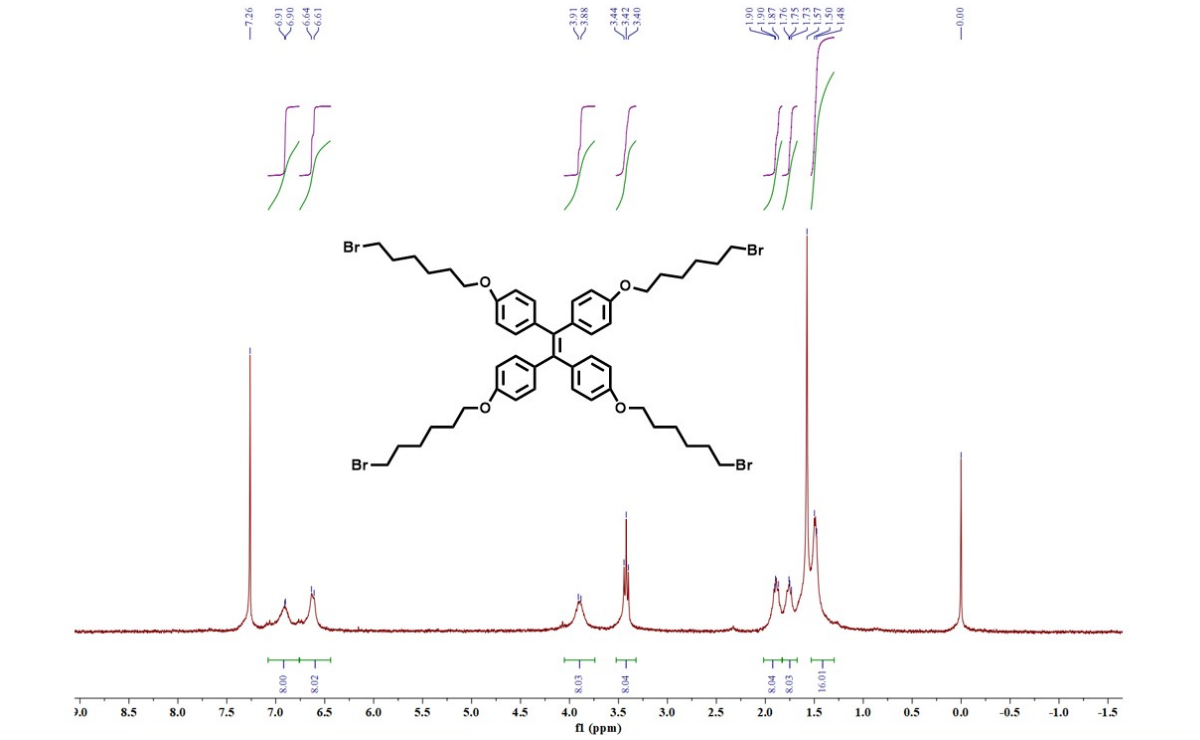

Figure S10 ^{1}H-NMR spectrum of molecule **3** in $CDCl_3$.

2.3 Supplementary NMR spectra of H_1, H_3 and G

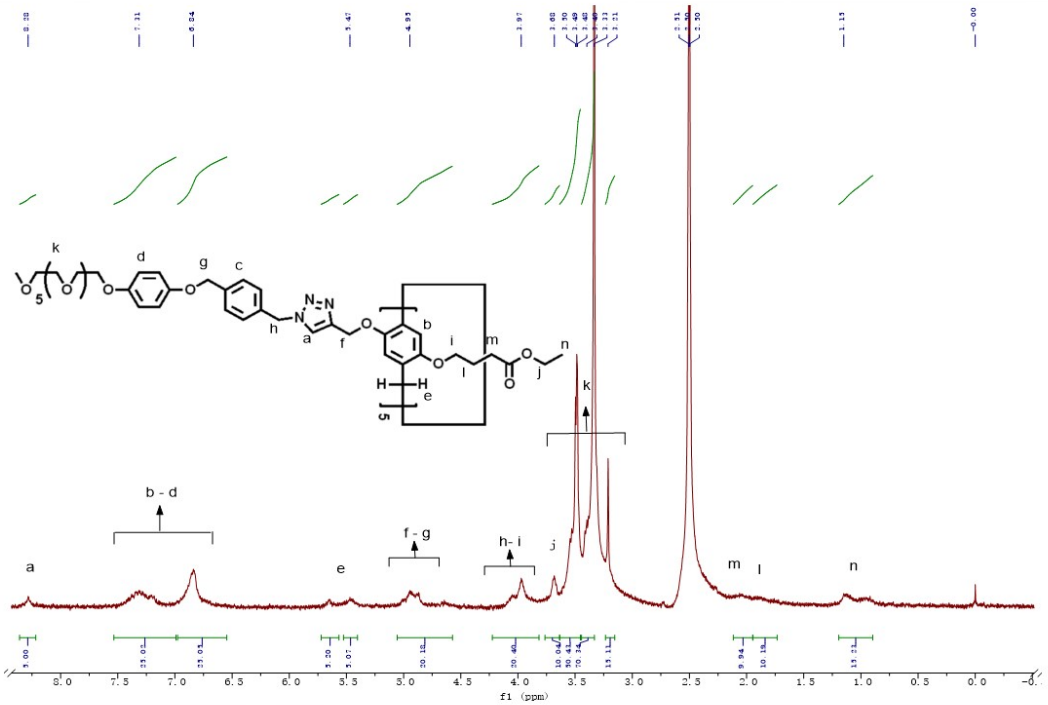

Figure S11 ^{1}H-NMR spectrum of molecule $\mathbf{H_1}$ in DMSO-d_6.

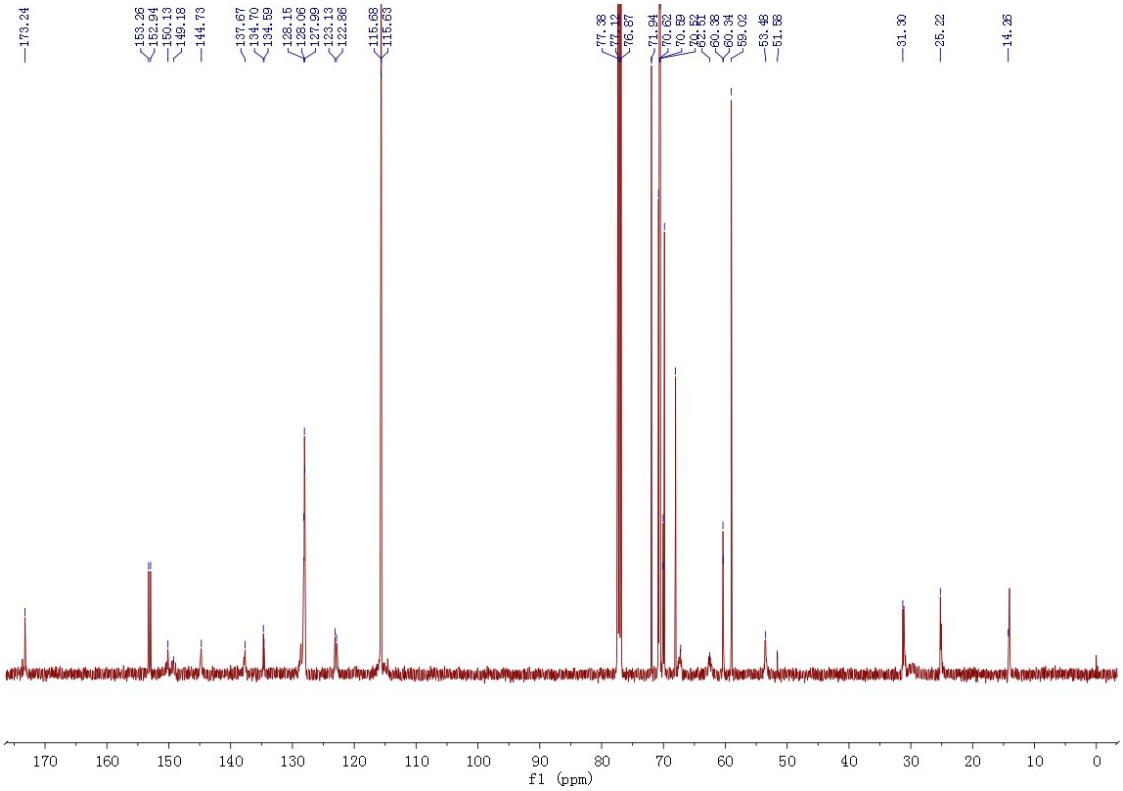

Figure S12 ^{13}C-NMR spectrum of molecule $\mathbf{H_1}$ in $CDCl_3$.

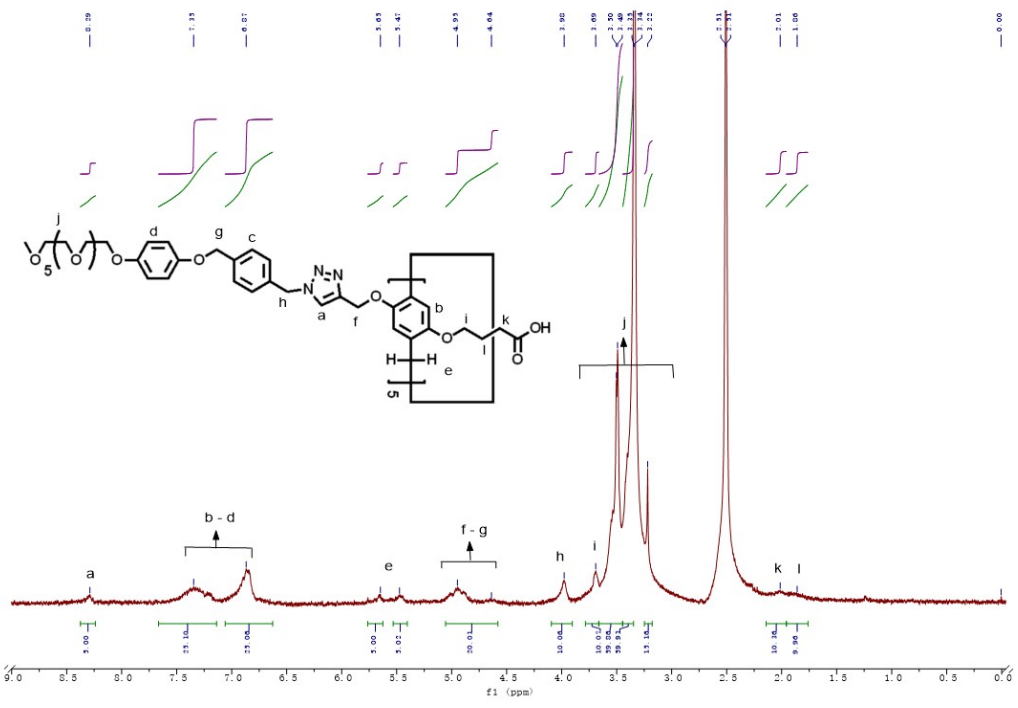

Figure S13 ^{1}H-NMR spectrum of molecule $\mathbf{H_3}$ in DMSO-d_6.

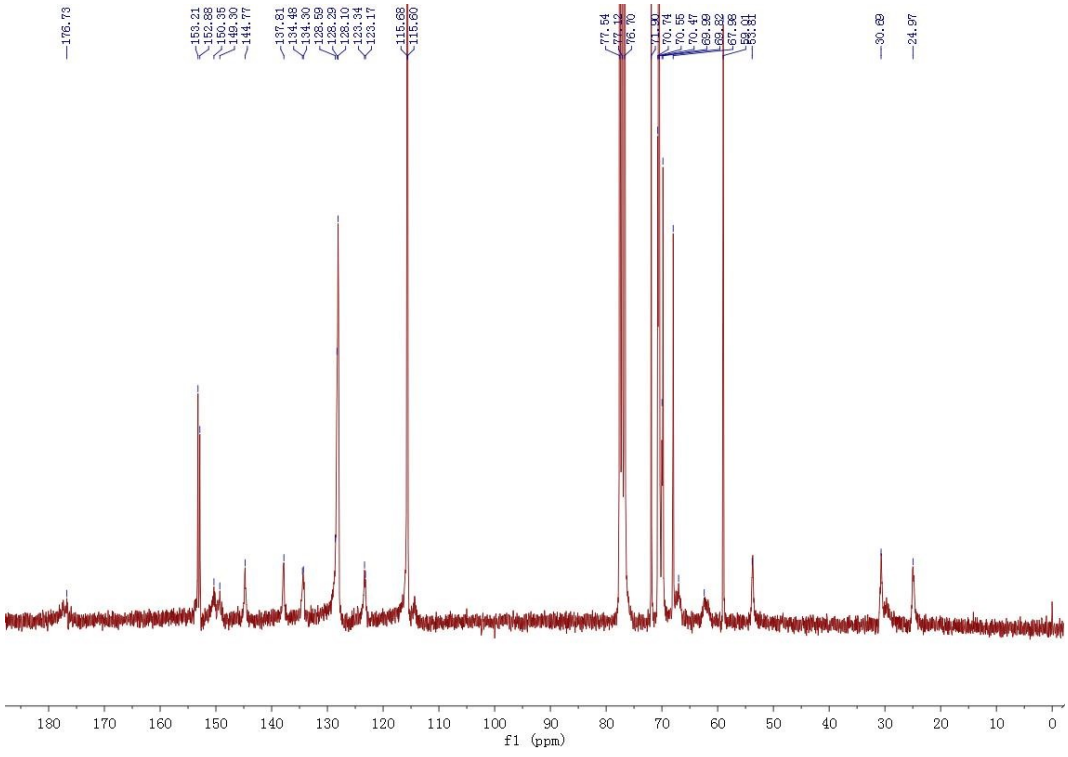

Figure S14 ^{13}C-NMR spectrum of molecule $\mathbf{H_3}$ in $CDCl_3$.

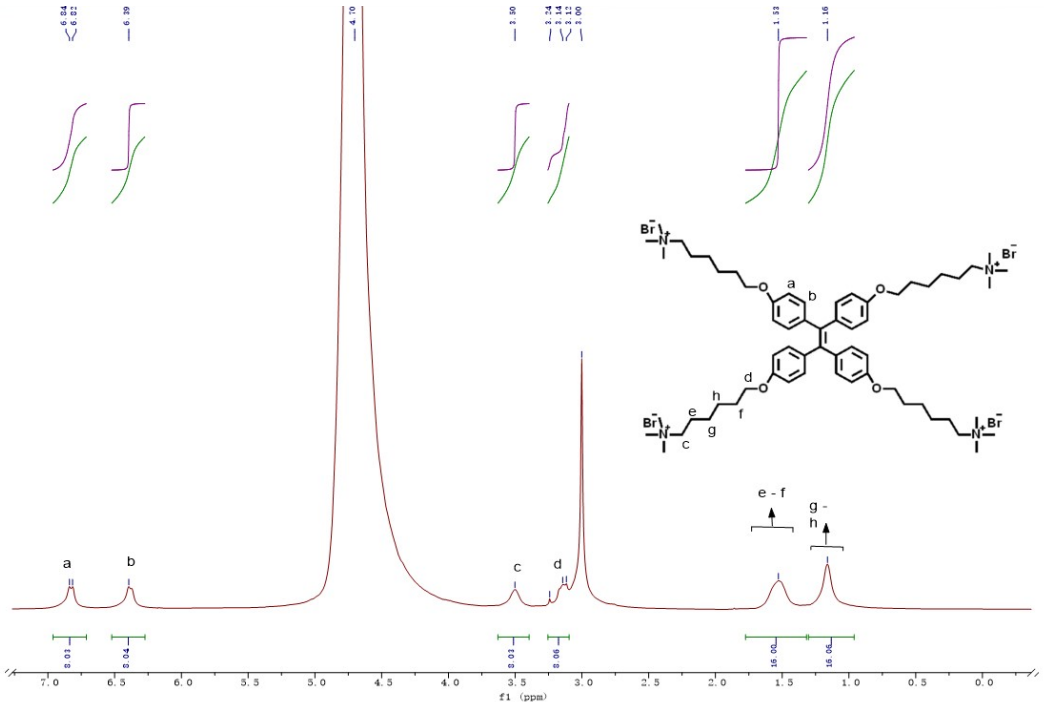

Figure S15 ^{1}H-NMR spectrum of molecule **G** in D2O.

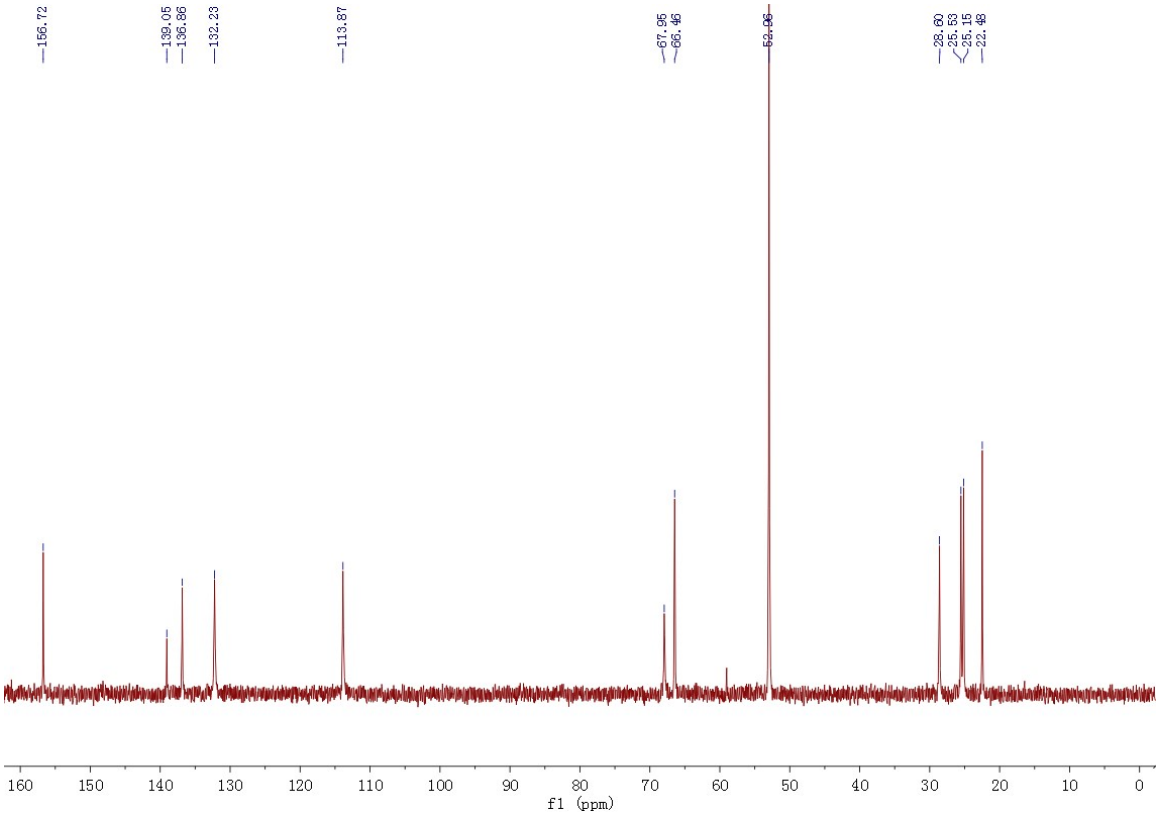

Figure S16 ^{13}C-NMR spectrum of molecule **G** in D2O.

2.4 Supplementary MS spectra of H_1, H_3.

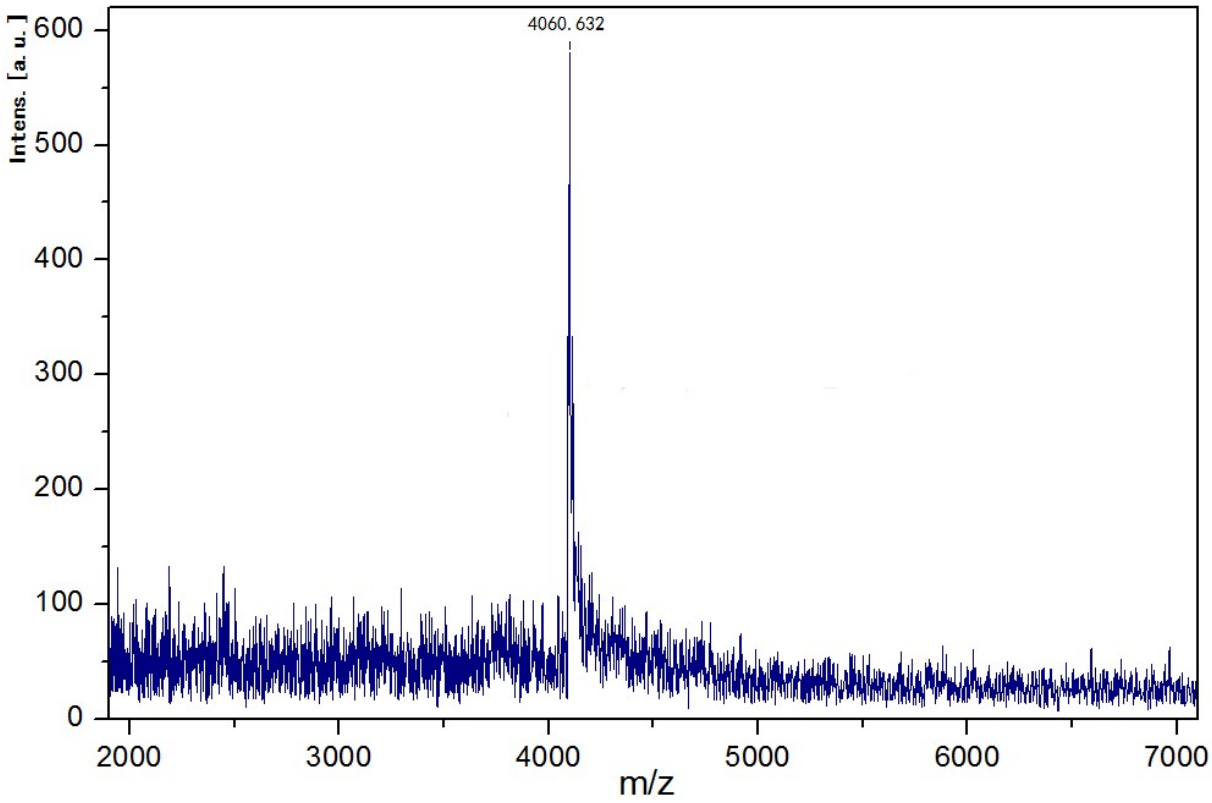

Figure S17 MALDI-TOF-Mass spectra of molecule $\mathbf{H_1}$.

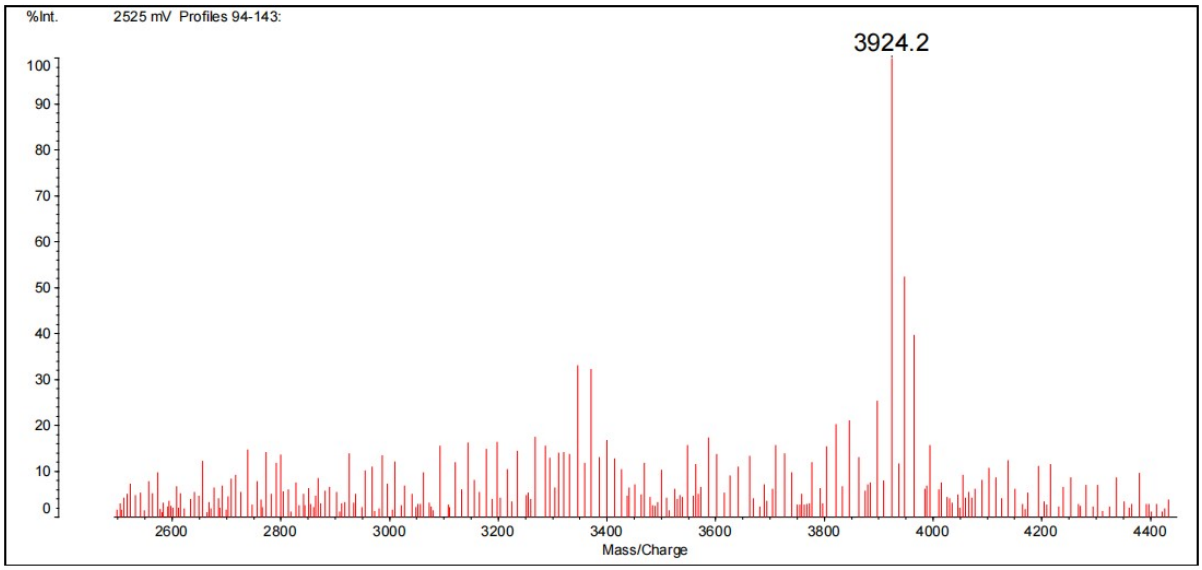

Figure S18 MALDI-TOF-Mass spectra of molecule $\mathbf{H_3}$.

3. Results and Discussion

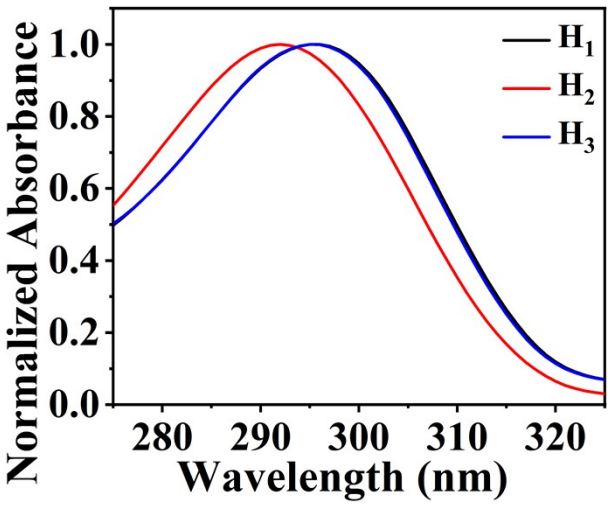

Figure S19 The normalized absorption spectrum of $\mathbf{H_1}$, $\mathbf{H_2}$ and $\mathbf{H_3}$ in aqueous solution.

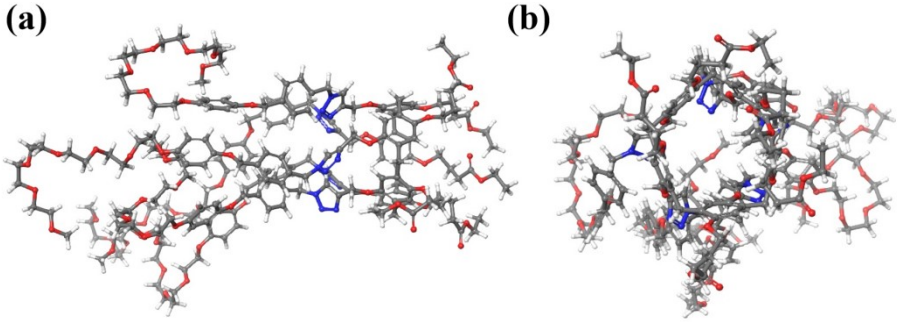

Figure S20 (a) The images of molecular dynamic simulation results of $\mathbf{H_1}$ in aqueous solution; (b) the top view of (a).

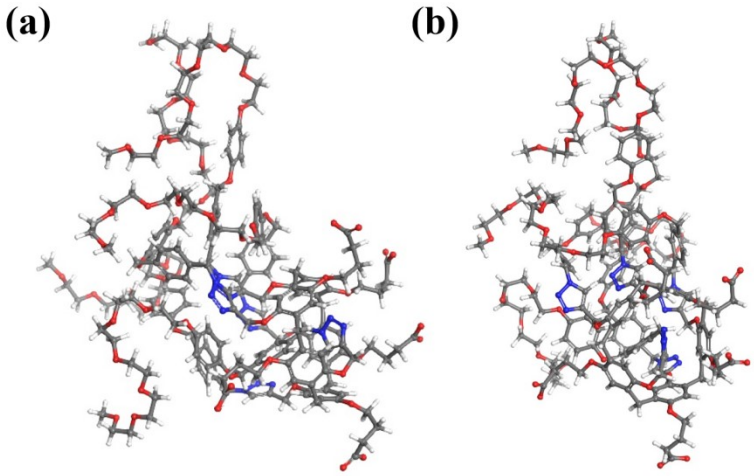

Figure S21 (a) The images of molecular dynamic simulation results of $\mathbf{H_2}$ in aqueous solution; (b) the top view of (a).

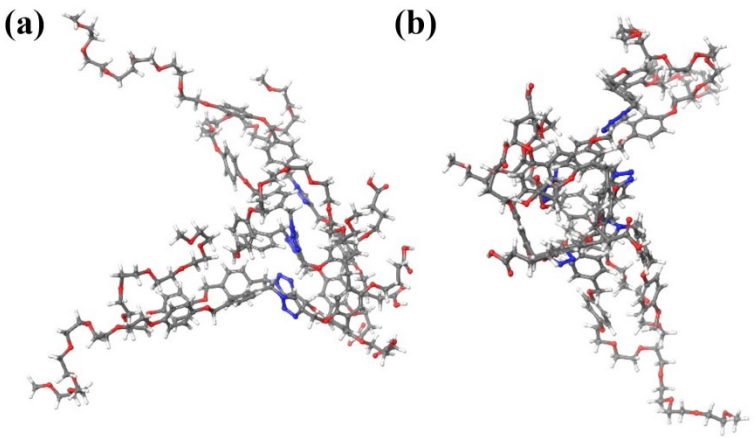

Figure S22 (a) The images of molecular dynamic simulation results of $\mathbf{H_3}$ in aqueous solution; (b) the top view of (a).

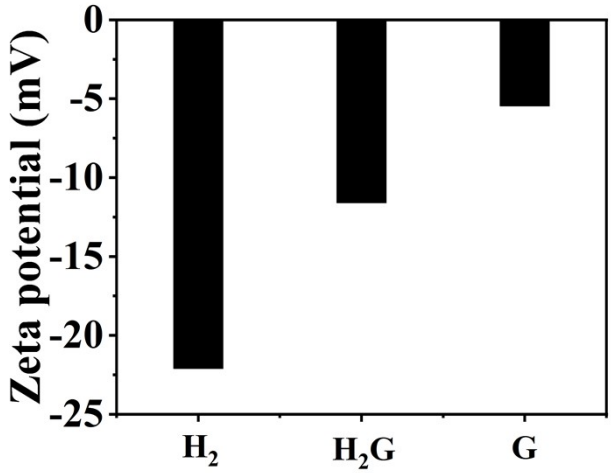

Figure S23 The zeta potentials of $\mathbf{H_2}$, $\mathbf{H_2G}$ and **G**.

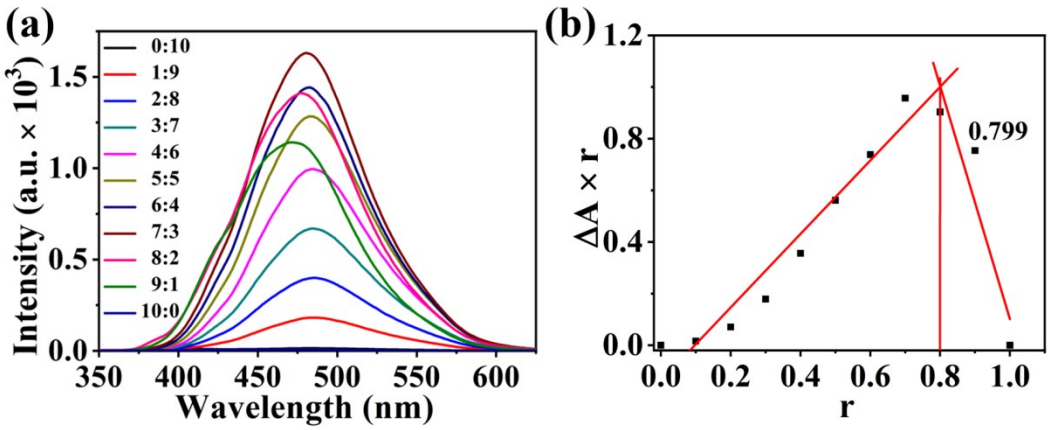

Figure S24 (a) Fluorescent spectra of the complex of $\mathbf{H_2}$ and **G** (curves from top to

bottom, molar ratios from 0 : 10 to 10 : 0) in aqueous solution, excited at 343 nm. (b) Job's plot of $\Delta A \times r$ vs r detected by fluorescent intensity at 484 nm.

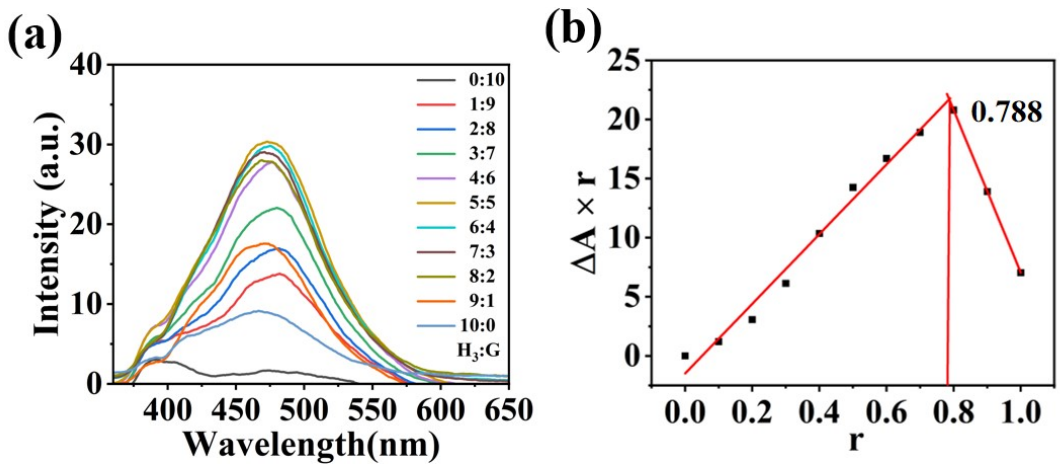

Figure S25 (a) Fluorescent spectra of the complex of $\mathbf{H_3}$ and **G** (curves from top to bottom, molar ratios from 0 : 10 to 10 : 0) in aqueous solution, excited at 343 nm. (b) Job's plot of $\Delta A \times r$ vs r detected by fluorescent intensity at 479 nm.

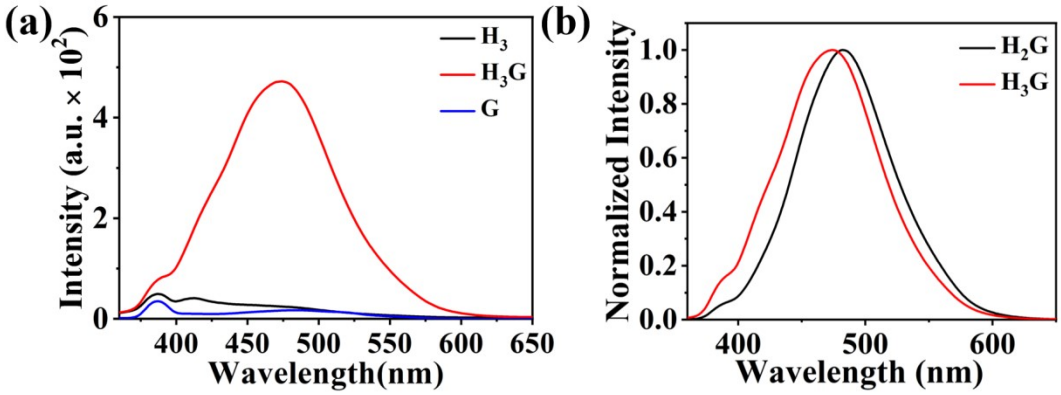

Figure S26 (a) Fluorescence spectra of $\mathbf{H_3}$, **G** and $\mathbf{H_3G}$; (b) The normalized fluorescence intensity of $\mathbf{H_2G}$ and $\mathbf{H_3G}$ in aqueous solution.

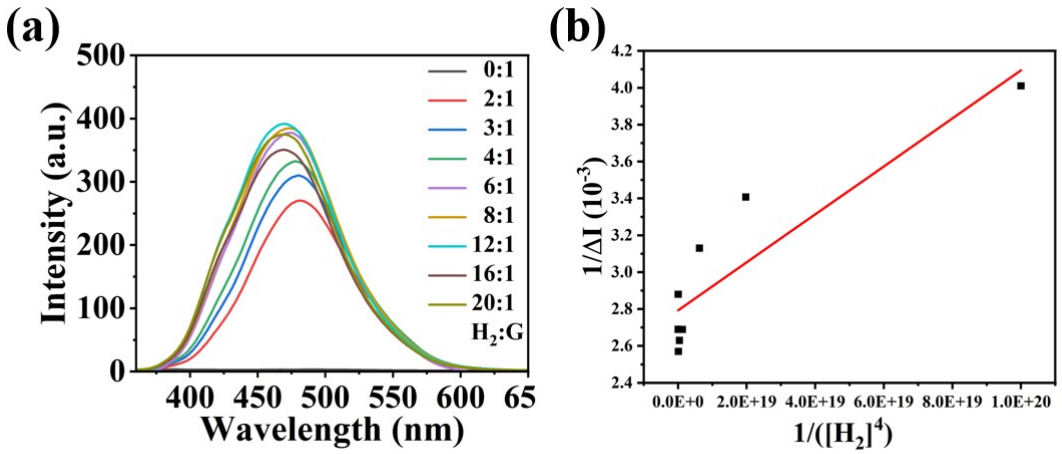

Figure S27 (a) Fluorescent spectra of the complex of $\mathbf{H_2}$ and **G** (curves from top to bottom, molar ratios = 0 : 1, 2 : 1, 3 : 1, 4 : 1, 6 : 1, 8 : 1, 12 : 1, 16 : 1, 20:1) in aqueous solution. (b) The plot of 1/ Δ I vs 1/ $[\mathbf{H_2}]^4$ detected by fluorescent intensity at 469 nm. Ka = 2.56×10^{20} M^{-4}.

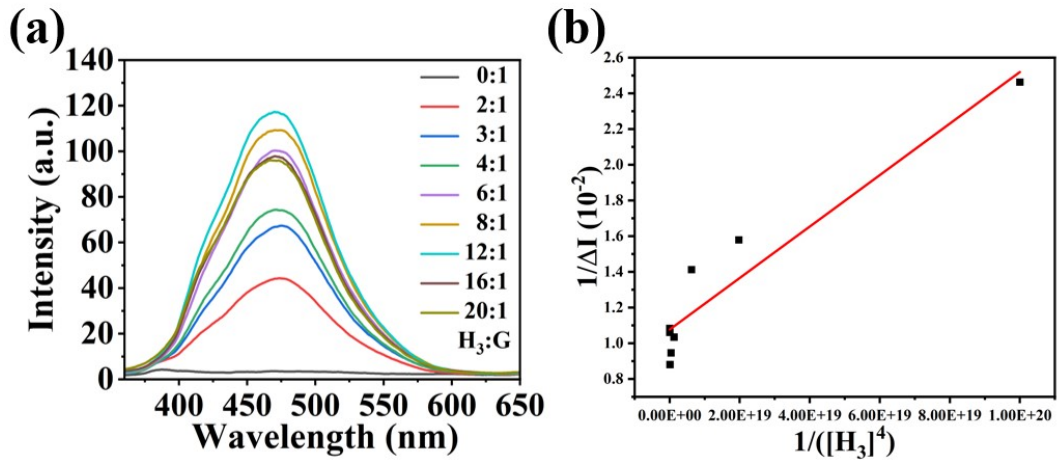

Figure S28 (a) Fluorescent spectra of the complex of $\mathbf{H_3}$ and **G** (curves from top to bottom, molar ratios = 0 : 1, 2 : 1, 3 : 1, 4 : 1, 6 : 1, 8 : 1, 12 : 1, 16 : 1, 20:1) in aqueous solution. (b) The plot of 1/ Δ I vs 1/ $[\mathbf{H_3}]^4$ detected by fluorescent intensity at 471 nm. Ka = 8.03×10^{19} M^{-4}.

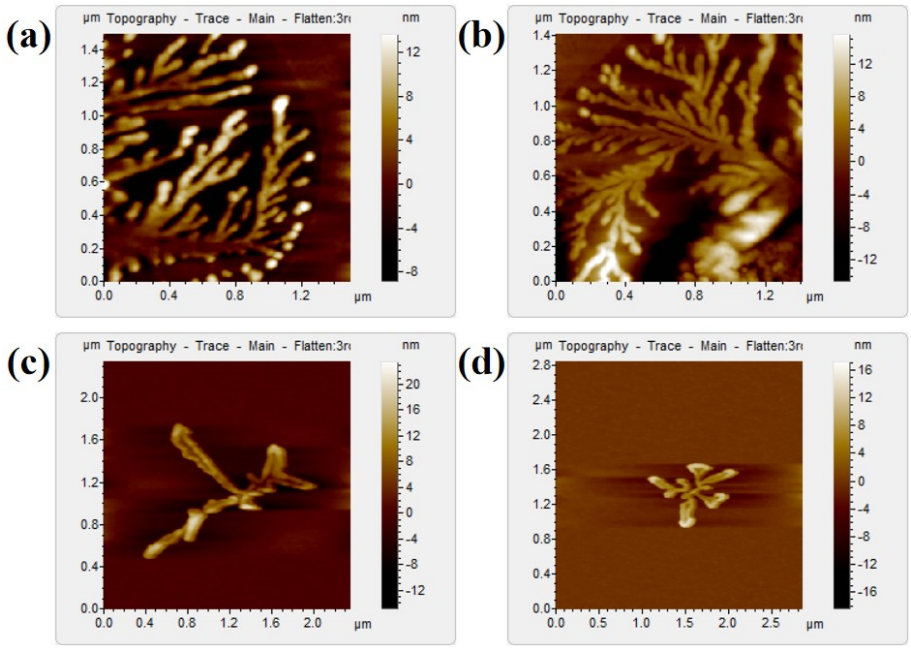

Figure S29 The Original AFM images with scale bars directly provided by instruments in aqueous solutions: (a) and (b) $\mathbf{H_2G}$, (c) and (d) $\mathbf{H_3G}$.

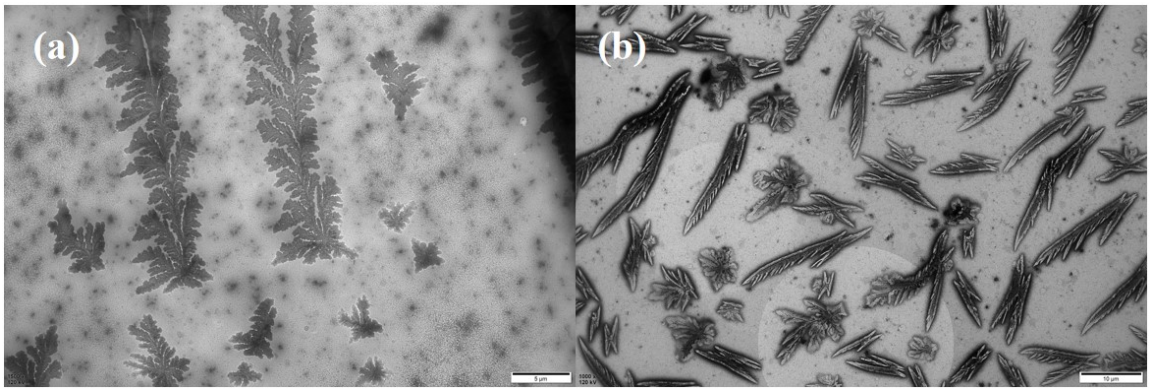

Figure S30 The Original TEM images with scale bars directly provided by instruments in aqueous solutions: (a) $\mathbf{H_2G}$, (b) $\mathbf{H_3G}$.

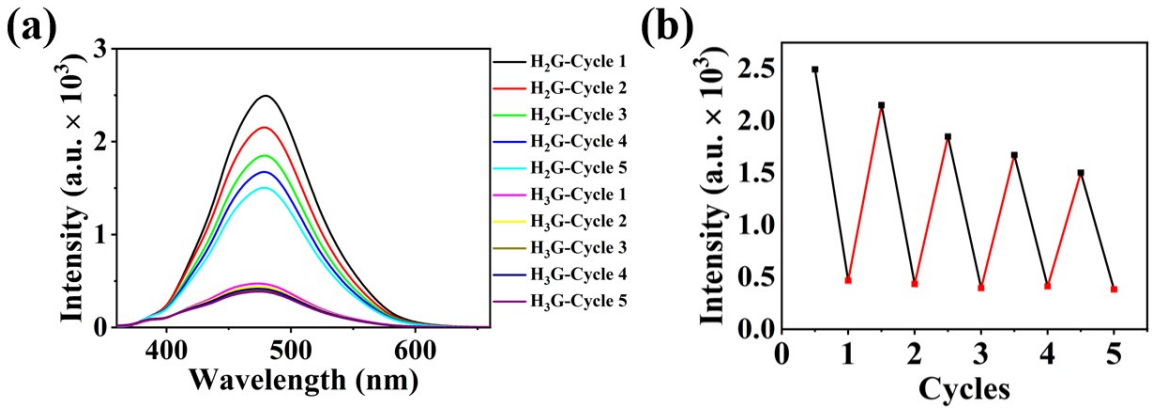

Figure S31 (a) Fluorescence spectra of **H_2G** and **H_3G** in aqueous solution with different pH cycles; (b) Fluorescence intensity of **H_2G** at 480 nm under alternate pH for 5 cycles.

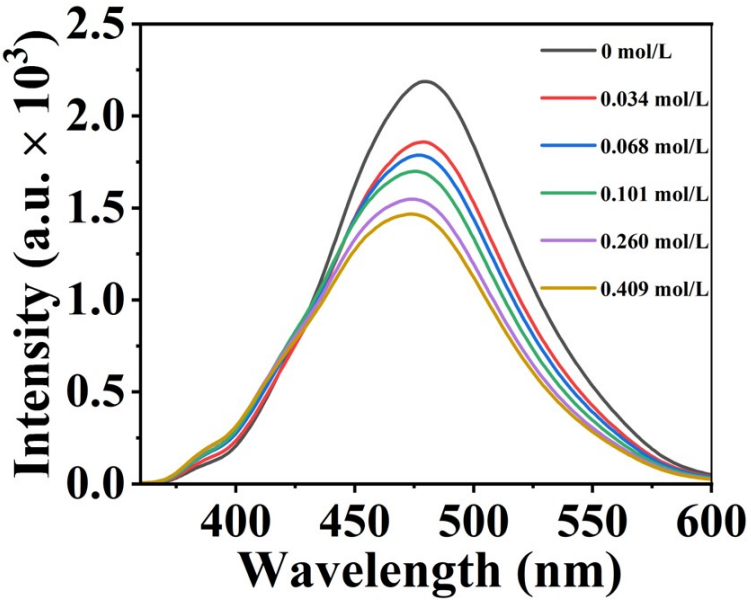

Figure S32 Fluorescence spectra of **H_2G** in aqueous solution with different concentration of NaCl.

4. References

S1. P. Liu, Y. Deng, J. Lu, X. Gou, Q. Han, Y.-R. Pei and L. Y. Jin, *Polym. Int*. 2024, **73**, 359-367.

S2. P. Wang, X. Yan and F. Huang, *Chem. Commun*. 2014, **50**, 5017-5019.